CHAOS
Theory and Applications
in Applied Sciences and Engineering

e-ISSN: 2687-4539
RESEARCH ARTICLE
Vol.6 / No.3 / 2024 / pp.159-169
https://doi.org/10.51537/chaos.1448912

Birth of Catastrophe and Strange Attractors through Generalized Hopf Bifurcations in Covid-19 Transmission Mathematical Model

Ario Wiraya *,1, **Yudi Ari Adi** α,2, **Laila Fitriana** *,3, **Triyanto** *,4, **Yuvita Andriani Kusumadewi** *,5, **Azimatus Nur Safitri** *,6 **and Aulia Nurmalitasari** *,7

*Universitas Sebelas Maret, Surakarta (UNS), 57126, Indonesia, αUniversitas Ahmad Dahlan, Yogyakarta, 55166, Indonesia.

ABSTRACT Coronavirus can be transmitted through the things that people carry or the things where it sticks to after being spread by the sufferer. Instead, various preventive measures have been carried out. We create a new mathematical model that represents Coronavirus that exists in non-living objects, susceptible, and infected subpopulations interaction by considering the Coronavirus transmission through non-living objects caused by susceptible and infected subpopulations along with its prevention to characterize the dynamics of Coronavirus transmission in the population under those conditions. One disease-free and two infection equilibrium points along with their local stability and coexistence are identified. Global stability of the disease-free equilibria and basic reproduction number are also investigated. Changes in susceptible-Coronavirus interaction rate generate Fold and Hopf bifurcations which represent the emergence of a cycle and the collision of two infection equilibrium points respectively. Catastrophe generated by the collision between an attractor and a repeller is found around a Generalized Hopf bifurcation point by changing susceptible-Coronavirus interaction rate and increasing rate of Coronavirus originating from infected subpopulation. It represents a momentary unpredictable dynamics as the effect of Coronavirus addition and infection. Non-chaotic strange attractors that represent complex but still predictable dynamics are also triggered by Generalized Hopf bifurcation when the susceptible-Coronavirus interaction rate and one of the following parameters, i.e. increasing rate of Coronavirus originating from infected subpopulation or infected subpopulation recovery rate vary.

KEYWORDS
Covid-19
Catastrophe
Generalized hopf
Strange attractor

INTRODUCTION

Covid-19 case was reported on the 31st of December 2019 in China (He *et al.* 2020; Zu *et al.* 2020). Covid-19 is a dangerous disease caused by Coronavirus (Pedersen and Ho 2020). Globally, as of April 23, 2023, there have been 764 million Covid-19 incidences which consist of 6 million death cases (WHO 2020). The most common form of Covid-19 transmission is direct contact transmission. The transmission occurs when interactions between an infected person and a susceptible person such as physical contact and contagion through air droplets exist. Things or non-living media exposed to the virus are also included as media of Covid-19 transmission (Ramesh *et al.* 2020).

There are several experiments have been carried out to analyze the lifecycle of Coronavirus as follows (van Doremalen *et al.* 2020). In aerosols, Coronavirus can survive for 3 hours. Coronavirus can not survive on copper after 4 hours. No viable Coronavirus was found on carton after 24 hours. On plastic and stainless steel, Coronavirus can survive better until 72 hours. Coronavirus can survive on different surfaces of various materials, such as paper, glass, PVC, metal, ceramic, and teflon until 5 days (Carraturo *et al.*

Manuscript received: 9 March 2024,
Revised: 25 May 2024,
Accepted: 10 June 2024.

[1]ariowiraya@staff.uns.ac.id (**Corresponding author**)
[2]yudi.adi@math.uad.ac.id
[3]lailafitrianafkip@staff.uns.ac.id
[4]triyanto.math@staff.uns.ac.id
[5]yuvitaandriani@student.uns.ac.id
[6]azimatusnur@student.uns.ac.id
[7]aulianurmalitasari16@student.uns.ac.id

2020). It provides critical information about the stability of Covid-19 and it is still possible for the virus to infect people after touching contaminated non-living media.

Asymptomatic and presymptomatic conditions also become an important factor in the Covid-19 spread. These silent carrier factors cause a dangerous impendence to Covid-19 treatment efforts for the precaution and countermeasures of Covid-19 since it is not detected (Obi and Odoh 2021). Even though the pandemic has been overcome in several countries, specific therapeutics and vaccines have not yet been found, while continuous spread by silent carrier factors could cause the incidence of these cases to increase again. Transmission of the silent carriers could be minimized by using face masks, maintaining social distancing, hand washing and sanitizing regularly, and avoiding crowds of people (Vermund and Pitzer 2021; for Disease Prevention and Control 2020; Gandhi *et al.* 2020). These imply that the transmission of Covid-19 also considers susceptible subpopulations and Coronavirus eradication efforts.

Mathematical modeling is an important tool to characterize and predict dynamics occurring in a system. Some researchers used it in many applications as follows. In the field of Biology, analysis of the predator-prey mathematical model reveals the extinction of prey or predator in a population (Mondal *et al.* 2024), the potential for environmental or human disturbance effects (Sk *et al.* 2023), the effects of species memory on the system (Thirthar *et al.* 2023), and the effects of additional food for the predator (Thirthar 2023). In the other fields, i.e. Economics and Environment, mathematical modeling is used to determine a strategy of inventory management in order to reduce global warming and carbon emission (Pakhira *et al.* 2024).

Until now, many researchers have constructed numerous models for Covid-19 by using the concepts of differential equations systems, such as the SIR mathematical model to characterize Covid-19 transmission. A mathematical model of Coronavirus infection in a population has been constructed (AlQadi and Bani-Yaghoub 2022). The research studies the interaction between susceptible, infected, and recovery subpopulations, but it has not considered the infection from Coronavirus that exists on non-living objects and its prevention. Another research is also conducted (Din and Algehyne 2021). They develop a mathematical model of Coronavirus transmission by considering the prevention of Coronavirus transmission. However, it still has not considered the infection from Coronavirus that exists on non-living objects. Other research has also been conducted by (Yang and Wang 2020) that reveals the effect of exposed and Coronavirus subpopulation addition to the system. The research has considered the infection from Coronavirus that exists on non-living objects. Meanwhile, it has not considered susceptible subpopulation as one of the Coronavirus carriers. It also has not considered the prevention of the infection from Coronavirus that exists on non-living objects.

Based on the previous studies that have not considered these three following factors together, i.e. the infection from Coronavirus that exists on non-living objects, susceptible subpopulation as one of the Coronavirus carriers, and the prevention of the infection from Coronavirus that exists on non-living objects, we create and analyze a new mathematical model, i.e. nonlinear ordinary differential equations system by considering those three factors to characterize the dynamics under those conditions so that the conditions of some important phenomena that should be reached or avoided can be revealed and become a medical recommendation to overcome Covid-19 in the population.

This research is conducted by explaining the motivation, state of the art, and novelty of this article in the introduction, constructing the mathematical model, analyzing the positivity, and boundedness of the model solution, equilibrium points, basic reproduction number, coexistence and local stability of the equilibrium points, and the bifurcations which consist of some phenomena such as strange attractors and catastrophe dynamics. Characterization of Covid-19 transmission shown by the phenomena becomes the indicator to predict the dynamics in the population as the parameters vary.

MATHEMATICAL MODEL

Development of the mathematical model is started by identifying the subpopulations that interact with each other in the population along with the assumption to limit the scope of this research. Based on the conditions which have been explained, there are three subpopulations which interact with each other in the population, i.e. Coronavirus that exists in non-living objects, susceptible, and infected subpopulations. In this research, we assume that the eradication of Coronavirus that exists in non-living objects is ignored and an increase in the number of Coronavirus that exists in non-living objects due to infected subpopulation has the same value as the number of infectious units of the Coronavirus enumerated by a plaque assay (Sender *et al.* 2021).

After identifying the subpopulations that interact with each other in the population along with the assumption, we define the subpopulations as the variables in the mathematical model. Definition of the variables are written in the Table 1. V, S, and I denote subpopulations and t denotes time so that they are nonnegative.

Table 1 Variables in the Model

Variable	Definition	Initial Value	Unit
V	Coronavirus subpopulation attached to non-living media	Estimation	virion
S	Susceptible subpopulation	Estimation	person
I	Infected subpopulation	Estimation	person
t	Time	Estimation	day

Every subpopulation in the population which is defined as the variable in the mathematical model interacts with each other. The level of each interaction is defined as the parameters in the mathematical model. Definition of the parameters are written in the Table 2. The initial value for several parameters were set in accordance with the previous research, while the initial values for several other parameters were assumed because the data had not been found either from primary sources, or from the previous research. All of the parameters have a positive value. We define d as the difference between infection of Coronavirus that exists in non-living objects and the prevention rate of the infection from Coronavirus that exists on non-living objects, i.e. $d = p - q$. The parameter d is possible to be negative if the infection of Coronavirus that exists in

Table 2 Parameters in the Model

Parameter	Definition	Value	Unit	Reference
a	Coronavirus increasing rate from infected subpopulation	100	virion per day	(Sender *et al.* 2021)
b	Coronavirus death rate	1	virion per day	(Yang and Wang 2020)
c	Susceptible subpopulation natural birth rate	10.7	person per day	(Din and Algehyne 2021)
p	Infection of Coronavirus that exists in non-living objects rate	1	virion per day	Assumption
q	Prevention rate of Coronavirus that exists in non-living infection	0.5	virion per day	Assumption
m	Coronavirus increasing rate from suspected subpopulation	0.5	virion per day	Assumption
e	Susceptible subpopulation natural death rate	0.0062	per day	Assumption
f	Infected subpopulation recovery rate	1	per day	(AlQadi and Bani-Yaghoub 2022)
g	Susceptible-infected interaction rate	0.0707	per day	(Din and Algehyne 2021)
h	Infected subpopulation death rate due to Coronavirus infection	0.02	person per day	(Din and Algehyne 2021)

non-living objects rate (p) is less than its prevention rate (q).

According to the model variables and parameters that have been written, we illustrate the interaction between the variables with the parameters as the rate in Figure 1.
According to the transfer diagram in Figure 1, we create a system of nonlinear ordinary differential equations as a mathematical model that represents the interaction, i.e.

$$\frac{dV}{dt} = aI - bV + mS \tag{1}$$

$$\frac{dS}{dt} = c - dSV - eS + fI - gSI \tag{2}$$

$$\frac{dI}{dt} = dSV + gSI - fI - hI \tag{3}$$

Equation (1) represents the rate of change of the virus population with respect to time which is denoted by aI as the coronavirus addition from infected subpopulation, because they sneeze, or the other reason, bV as coronavirus death, and mS as the coronavirus addition from suspected subpopulation because they carried.

Equation (2) represents the rate of change in the susceptible population with respect to time. The first term is the increase of susceptible population caused by the susceptible population's natural birth by c. The second term is the reduction of the susceptible population due to its interaction with the virus, in which d denotes the interaction rate. The third term is the reduction of susceptible population caused by the susceptible population's natural

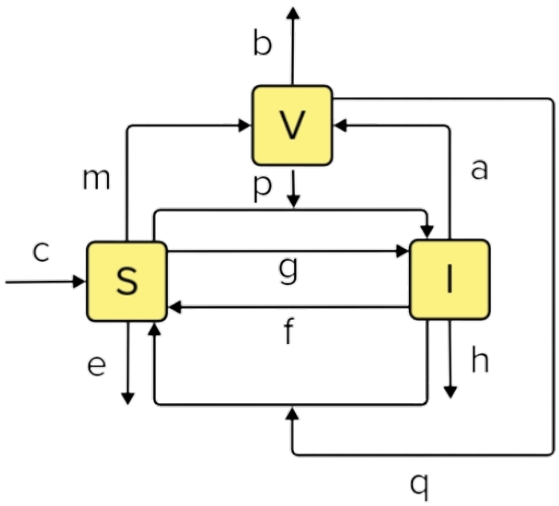

Figure 1 Transfer diagram of the interaction between Coronavirus, susceptible, and infected subpopulations.

death with e as its rate. The fourth term is the increase of susceptible population caused by the infected population recovery where f represents the rate. The fifth term is reducing the susceptible population due to its interaction with the infected population with g as its rate.

Equation (3) represents the rate of change in the infected population with respect to time. The first term is the increase in the infected population due to the interaction between the susceptible population and the virus where d denotes the interaction rate. The second term is the increase in the infected population caused by its interaction with the susceptible population by g. The third term is the reduction of the infected population caused by the infected population recovery, where f represents the rate. The fourth term is the reduction of the infected population caused by the infected population death due to Coronavirus with h as its rate.

POSITIVITY AND BOUNDEDNESS OF SOLUTION

Solution of the model must be positive in order to get the biological interpretation (Wiraya *et al.* 2022). The following theorem guarantees the positivity of the solution.

Theorem 1. The solution set $\{V, S, I\}$ of the model with non-negative initial condition $V(0) = V_0$, $S(0) = S_0$, and $I(0) = I_0$ remain non-negative for all time $t > 0$.

Proof. For the non-negative initial condition $V(0) = V_0$, $S(0) = S_0$, and $I(0) = I_0$, it is clear from the Equation (1) that $\frac{dV}{dt} + bV(t) \geq 0$, so that $\frac{d}{dt}\left[V(t)e^{bt}\right] \geq 0$. By integrating the last inequality, we obtain $V(t) \geq V(0)e^{-bt} > 0$ for all $t > 0$. Further, from Equation (2), we get $\frac{dS}{dt} + [dV(t) + e + gI(t)]S(t) \geq 0$, so that $S(t) \geq S(0)e^{-(et+d\int_0^t V(\tau)d\tau + g\int_0^t I(\tau)d\tau)} > 0$ for all $t > 0$. Similarly, it can be shown that $I(t) > 0$ for all $t > 0$.

Besides the positivity, the solution of the model must also be bounded, so that it has a biological meaning (Wiraya *et al.* 2022). Boundedness of the solution is guaranteed by the following theorem.

Theorem 2. Every solution of the model initiated in $\mathbb{R}^3_+$ is bounded.

Proof. By subtracting Equation (2) and Equation (3), we have $\frac{d}{dt}[S(t) + I(t)] = c - eS - hI \leq c - p[S(t) + I(t)]$, where $p = \min\{e, h\}$. Therefore $S(t) + I(t) \leq \frac{c}{p} + \left[S(0) + I(0) - \frac{c}{p}\right]e^{-pt}$. Hence, $S(t) + I(t) \to \frac{c}{p}$ as $t \to \infty$. Thus, $S(t)$ and $I(t)$ are bounded. Furthermore, from Equation (1), we get $\frac{dV}{dt} = aI - bV + mS \leq aI + mS \leq q[S(t) + I(t)]$, where $q = \max\{a, m\}$. Hence, $V(t)$ is bounded since $S(t)$ and $I(t)$ are bounded. Therefore, $V(t)$, $S(t)$, and $I(t)$ are bounded in $\mathbb{R}^3_+$.

EQUILIBRIUM POINTS

The equilibrium point represents a steady state condition of each subpopulation number over time. Consider $a_2 = gb^2eh$, $a_1 = (dbh - (f+h))(ae - mh) - gcb(ae + mh)$, $a_0 = gac^2m - ((f+h)mc + dac)(ae - mh)$. The equilibrium point of the model is explained in the following theorem.

Theorem 3. Equilibrium points of the system are

$$E_1 = \left(V_1^*, \frac{ac - bhV_1^*}{ae - mh}, \frac{ebV_1^* - mc}{ae - mh}\right)$$

and

$$E_2 = \left(V_2^*, \frac{ac - bhV_2^*}{ae - mh}, \frac{ebV_2^* - mc}{ae - mh}\right),$$

where

$$V_1^* = \frac{-a_1 + \sqrt{a_1^2 - 4a_2a_0}}{2a_2}$$

and

$$V_2^* = \frac{-a_1 - \sqrt{a_1^2 - 4a_2a_0}}{2a_2}$$

If $V_1^* = V_2^* = \frac{mc}{eb}$, then there is one disease-free equilibria, i.e. $E_1 = E_2 = E_0 = (\frac{mc}{eb}, \frac{c}{e}, 0)$. On the other condition, the system has two infection equilibrium points, i.e. E_1 and E_2.

Proof. The equilibrium points E^* are solutions of the model when Equation (1) = Equation (2) = Equation (3) = 0 (Wiggins 2003; Wiraya and Adi-Kusumo 2023), i.e.

$$aI - bV + mS = 0 \tag{4}$$

$$c - dSV - eS + fI - gSI = 0 \tag{5}$$

$$dSV + gSI - fI - hI = 0 \tag{6}$$

By adding Equation (5) and Equation (6), we found $c - eS - hI = 0$ which is equivalent to $I^* = \frac{c - eS}{h}$. By substituting I^** to Equation (4), we obtain $S^* = \frac{ac - bhV^*}{ae - mh}$. By substituting S^* to I^**, we found $I^* = \frac{ebV^* - mc}{ae - mh}$. By substituting S^* and I^* to Equation (6), we obtain a quadratic equation

$$a_2V^2 + a_1V + a_0 = 0. \tag{7}$$

Thus, we found that V_i^* for $i = 1, 2$ are the solutions of the quadratic equation, i.e. $V_1^* = \frac{-a_1 + \sqrt{a_1^2 - 4a_2a_0}}{2a_2}$ and $V_2^* = \frac{-a_1 - \sqrt{a_1^2 - 4a_2a_0}}{2a_2}$. Hence, $S_i^* = \frac{ac - bhV_i^*}{ae - mh}$ and $I_i^* = \frac{ebV_i^* - mc}{ae - mh}$, for $i = 1, 2$. Therefore, the equilibrium points are

$$E_1 = \left(V_1^*, \frac{ac - bhV_1^*}{ae - mh}, \frac{ebV_1^* - mc}{ae - mh}\right)$$

and

$$E_2 = \left(V_2^*, \frac{ac - bhV_2^*}{ae - mh}, \frac{ebV_2^* - mc}{ae - mh}\right).$$

Consider $V_1^* = V_2^* = \frac{mc}{eb}$, then we get $\frac{ebV_1^* - mc}{ae - mh} = \frac{ebV_2^* - mc}{ae - mh} = 0$ and $\frac{ac - bhV_1*}{ae - mh} = \frac{ac - bhV_1*}{ae - mh} = \frac{c}{e}$. Hence, we obtain $E_1 = E_2 = E_0 = (\frac{mc}{eb}, \frac{c}{e}, 0)$. It is a disease-free equilibria, because the infected subpopulation does not exist. Other than that condition, there are two infection equilibrium points, i.e. E_1 and E_2 since the infected subpopulation exists.

COEXISTENCE OF EQUILIBRIUM POINTS

The solution of the model must be real and positive in order to satisfy the existence of the equilibrium points. We see that $a_2 > 0$. We get different solutions depending on the signs of a_1 and a_0 that summarized in the following theorem.

Theorem 4. Consider one of the following conditions is fullfiled: i. $ae > mh$ and $\frac{mc}{eb} \leq V^* \leq \frac{ac}{bh}$; ii. $ae < mh$ and $\frac{ac}{bh} \leq V^* \leq \frac{mc}{eb}$. The System : a) has a unique equilibria if $a_0 < 0$; b) has two equilibrium if $a_0 > 0$ and $a_1 < 0$; c) has no equilibria if $a_0 > 0$ and $a_1 > 0$.

Proof. Consider the condition i or ii is fulfilled. Thus, S^* and I^* are non-negative. a) Consider $a_0 < 0$. We found that Equation (7) will have one positive and one negative value of V^*. Hence, the model has a unique equilibria. ii. Consider $a_0 > 0$ and $a_1 < 0$. Thus, Equation (7) will have two positive values of V^*. Hence, the model has two equilibrium points. iii. Consider $a_0 > 0$ and $a_1 > 0$. Hence, Equation (7) will have two negative values of V^*. Therefore, the model has no equilibria.

BASIC REPRODUCTION NUMBER

Transmission of a disease is determined by basic reproduction number. In this case, it becomes a parameter used to measure the potential of Coronavirus infection in a population.

Theorem 5. Basic reproduction number of the system is $R_0 = \frac{1}{2}(U + \sqrt{U^2 - 4W})$, where $U = \frac{c(bg-aq)}{be(f+h)}$ and $W = -\frac{ap}{b}$.

Proof. R_0 is calculated by using the Next Generation Matrix method (Castillo-Garsow and Castillo-Chavez 2020). R_0 is influenced by Equation (1) and Equation (3) because the Coronavirus infection originate from those equations. The positive and negative terms in those equations are grouped so that the following matrices are obtained.

$$\mu = \begin{pmatrix} aI + mS \\ pSV + gSI \end{pmatrix}, \psi = \begin{pmatrix} bV \\ qSV + fI + hI \end{pmatrix}.$$

Jacobian matrix of μ and ψ evaluated on E_0 are written as follows.

$$F = \begin{pmatrix} 0 & a \\ \frac{pc}{e} & \frac{gc}{e} \end{pmatrix}, G = \begin{pmatrix} b & 0 \\ \frac{qc}{e} & f+h \end{pmatrix}.$$

Hence, $G^{-1} = \begin{pmatrix} \frac{1}{b} & 0 \\ -\frac{qc}{be(f+h)} & \frac{1}{f+h} \end{pmatrix}$.

The Next Generation Matrix is

$$M = FG^{-1} = \begin{pmatrix} -\frac{aqc}{be(f+h)} & \frac{a}{f+h} \\ \frac{pce(f+h)-gqc^2}{be^2(f+h)} & \frac{gc}{e(f+h)} \end{pmatrix}.$$

The characteristic equation of M is

$$\lambda^2 + U\lambda + W = 0, \tag{8}$$

where λ is the eigen value of M, $U = \frac{c(bg-aq)}{be(f+h)}$, and $W = -\frac{ap}{b}$. Therefore, the eigenvalue of M are

$$\lambda_{1.2} = \frac{1}{2}(U \pm \sqrt{U^2 - 4W}).$$

Since the basic reproduction number is the largest eigenvalue (spectral radius) of M, we found that $R_0 = \frac{1}{2}(U + \sqrt{U^2 - 4W})$.

LOCAL STABILITY ANALYSIS

Local stability of the equilibrium points represents the convergence of the number of Coronavirus, susceptible, and infected subpopulations when the initial conditions of them are around the equilibrium points. We predict the dynamic of each subpopulation starting around the equilibrium points by analyzing the local stability using Routh-Hurwitz criteria (Perko 2001).

Consider $A = gI_i^* + dV_i^* + b + e + f + h$, $B = g^2S_i^* + dgS_i^*V_i^* + (bg + fg + gh)I_i^* + dmS_i^* + (b+h)dV_i^* + be + bf + bh + ef + eh - adS_i^* - fgS_i^*$, and $C = (adg + bg^2 + dgm)S_i^* + bdgS_i^*V_i^* + bg(f + h)I_i^* + dhmS_i^* + bdhV_i^* + be(f+h) - adgS_i^*I_i^* - adeS_i^* - bgfS_i^*$ for $i = 1, 2$. Local stability of the equilibrium points E^* is stated in the following theorem.

Theorem 6. The equilibrium points E_i^* for $i = 1, 2$ are locally asymptotically stable if $A > 0$, $C > 0$, and $AB - C > 0$.

Proof. To determine the local stability of equilibrium points E_i^* for $i = 1, 2$, we compute the Jacobian matrix given by

$$J_{E_i^*} = \begin{pmatrix} -b & m & a \\ -dS_i^* & -dV_i^* - e - gI_i^* & f - gS_i^* \\ dS_i^* & dV_i^* + gS_i^* & -(f+h) \end{pmatrix}.$$

Consider λ is the eigenvalue of $J_{E_i^*}$. The characteristic equation of $J_{E_i^*}$ is

$$\lambda^3 + A\lambda^2 + B\lambda + C = 0. \tag{9}$$

Based on the characteristic equation, we found that the equilibrium points E_i^* is locally asymptotically stable if $A > 0$, $C > 0$, and $AB - C > 0$ by using Routh-Hurwitz criteria.

We especially investigate the conditions that make the population free from Covid-19 which closely related to the disease-free equilibria stability condition. Local stability conditions of the disease-free equilibria are limited to the initial conditions of the subpopulations which are around the disease-free equilibria. Global stability conditions of the disease-free equilibria represent the criteria that should be fulfilled in order to make the population free from Covid-19 for any initial condition of the subpopulations.

GLOBAL STABILITY ANALYSIS

Global stability of the equilibrium points illustrates the convergence situation of the number of Coronavirus, susceptible, and infected subpopulations for any initial conditions of them. We especially analyze the global stabilty of $E_0 = \left(\frac{mc}{eb}, \frac{c}{e}, 0\right)$, i.e. the disease-free equilibria to obtain the conditions that make the population free from Covid-19 for any initial condition of the subpopulations. We analyze the dynamic of each subpopulation which can be started around or far from E_0 by using Lyapunov function (LaSalle and Lefschetz 1961). Global stability of the equilibrium points E_0 is stated in the following theorem.

Theorem 7. The disease-free equilibria E_0 is globally asymtotically stable if $p \le q$, $g \le e$, and $c \le f + h$.

Proof. We choose a function as follows.

$$L = Ie^{(S+I)}.$$

Hence, L and its first derivative is a continuous function on $\mathbb{R}^3_+$. For every $E = (V, S, I) \in \mathbb{R}^3_+$ and $E \neq E_0$, we obtain $L(E) > 0$. If $E = E_0$, then $L(E_0) = 0$. By using Equation (1), (2), and (3), the first derivative of L with respect to t is stated as follows.

$$\begin{aligned} \frac{dL}{dt} &= \frac{dI}{dt}e^{(S+I)} + Ie^{(S+I)}\left(\frac{dS}{dt} + \frac{dI}{dt}\right) \\ &= e^{(S+I)}\left[dSV + (g-e)SI - (f+h-c)I - hI^2\right], \end{aligned}$$

where $d = p - q$ by definition. Thus, $\frac{dL}{dt} \le 0$ if $p \le q$, $g \le e$, and $c \le f + h$.

BIFURCATION ANALYSIS

We vary some parameters of the model, i.e. susceptible-Coronavirus interaction rate (d), susceptible-infected interaction rate (g), infected subpopulation recovery rate (f), and Coronavirus increasing rate from infected subpopulation (a) and investigate its effect on the change of the number of equilibria and its stability to characterize the dynamics of Covid-19 transmission (Kuznetsov 1998).

Codimension-one Bifurcation

Fold and Hopf bifurcations occur when we make a E_2 as susceptible-Coronavirus interaction rate (d) decreases. The existence of Fold and Hopf bifurcations is presented analytically.

The existence of the Fold Bifurcation is written in the following theorem.

Theorem 8. Fold bifurcation occurs if $d = \frac{bg[(f-g)S_1^*-(f+h)I_1^*-(f+h)}{[a(g-e)+m(g+h)]S_1^*+(bV_1^*-aI_1^*)gS_1^*+bhV_1^*}$.

Proof. According to the theory in (Bosi and Desmarchelier 2019) and the characteristic Equation (9), we found that a Fold bifurcation occurs if $-C = 0$. It is equivalent with $d = \frac{bg[(f-g)S_1^*-(f+h)I_1^*-(f+h)}{[a(g-e)+m(g+h)]S_1^*+(bV_1^*-aI_1^*)gS_1^*+bhV_1^*}$.

The existence of the Non-neutral Hopf bifurcation is stated in the following theorem.

Theorem 9. Non-neutral Hopf bifurcation occurs if the value of d satisfies the quadratic equation $Pd^2 + Qd + R = 0$ where $P = (a-m)S_1^*V_1^* - (b+h)V_1^{*^2} - gS_1^*V_1^{*^2}$, $Q = (ag+gm-bm+ab-em-fm+fa+ah)S_1^* - (g^2+eg)S_1^*V_1^* - (2bf+ef+b^2+2bh+fh+h^2)V_1^* - mgS_1^*I_1^* - g^2S_1^*V_1^*I_1^* - (2bg+fg+2gh)V_1^*I_1^*$, and $R = (eg^2-efg+fg^2-f^g+hg^2-fhg)S_1^* + (bg^2+fg^2+g^2h+2beg+2gef+2geh+b^2g+2bfg+2bgh+f^2g+2fgh+gh^2)I_1^* + (g^3-fg^2)S_1^*I_1^* + b^2(e+f+h) + 2bef + 2beh + e^2(b+f+h) + (b+e)(f^2+h^2) + 2bfh + 2efh$.

Proof. According to the theory in (Bosi and Desmarchelier 2019) and the characteristic Equation (9), we found that Hopf bifurcations occur if $-C = B(-A)$. It is fulfilled if the value of d satisfies the quadratic equation $Pd^2 + Qd + R = 0$ where $P = (a-m)S_1^*V_1^* - (b+h)V_1^{*^2} - gS_1^*V_1^{*^2}$, $Q = (ag+gm-bm+ab-em-fm+fa+ah)S_1^* - (g^2+eg)S_1^*V_1^* - (2bf+ef+b^2+2bh+fh+h^2)V_1^* - mgS_1^*I_1^* - g^2S_1^*V_1^*I_1^* - (2bg+fg+2gh)V_1^*I_1^*$, and $R = (eg^2-efg+fg^2-f^g+hg^2-fhg)S_1^* + (bg^2+fg^2+g^2h+2beg+2gef+2geh+b^2g+2bfg+2bgh+f^2g+2fgh+gh^2)I_1^* + (g^3-fg^2)S_1^*I_1^* + b^2(e+f+h) + 2bef + 2beh + e^2(b+f+h) + (b+e)(f^2+h^2) + 2bfh + 2efh$.

Codimension-two Bifurcation

Codimension-two bifurcation is obtained through continuation of bifurcation point related to bifurcation value (Verhulst 1996) that found in codimension-one bifurcation. Some Generalized Hopf, Bogdanov-Takens, or Zero Hopf bifurcations are found when we make a continuation of the non-neutral Hopf bifurcation point as susceptible-Coronavirus interaction rate (d) and one of the following parameter, i.e. susceptible-infected interaction rate (g), infected subpopulation recovery rate (f), or Coronavirus increasing rate from infected subpopulation (a) vary. The existence of Bogdanov-Takens and Zero hopf bifurcations are explained analytically, but the existence of Generalized Hopf bifurcations are shown numerically, because of its complexity.

The existence of Bogdanov-Takens bifurcations is shown in the following theorem.

Theorem 10. Bogdanov-Takens bifurcations occur if $d = \frac{bg[(f-g)S_1^*-(f+h)I_1^*-(f+h)}{[a(g-e)+m(g+h)]S_1^*+(bV_1^*-aI_1^*)gS_1^*+bhV_1^*}$ and $d = \frac{(fg-g^2)S_1^*-g(b+f+h)I_1^*-b(e+f+h)-e(f+h)}{gS_1^*V_1^*+(m-a)S_1^*+(b+h)V_1^*}$.

Proof. According to the theory in (Bosi and Desmarchelier 2019) and the characteristic Equation (9), we found that Bogdanov-Takens bifurcations occur if $-C = 0$ and $-B = 0$. They are equivalent with $d = \frac{bg[(f-g)S_1^*-(f+h)I_1^*-(f+h)}{[a(g-e)+m(g+h)]S_1^*+(bV_1^*-aI_1^*)gS_1^*+bhV_1^*}$ and $d = \frac{(fg-g^2)S_1^*-g(b+f+h)I_1^*-b(e+f+h)-e(f+h)}{gS_1^*V_1^*+(m-a)S_1^*+(b+h)V_1^*}$ respectively.

The existence of Zero Hopf bifurcation is presented in the following theorem.

Theorem 11. Zero-Hopf bifurcation occurs if $d = \frac{bg[(f-g)S_1^*-(f+h)I_1^*-(f+h)}{[a(g-e)+m(g+h)]S_1^*+(bV_1^*-aI_1^*)gS_1^*+bhV_1^*}$, $d = -(gI_1^*+b+e+f+h)$, and $d > \frac{(fg-g^2)S_1^*-g(b+f+h)I_1^*-b(e+f+h)-e(f+h)}{gS_1^*V_1^*+(m-a)S_1^*+(b+h)V_1^*}$ where $gS_1^*V_1^* + (m-a)S_1^* + (b+h)V_1^* > 0$.

Proof. According to the theory in (Bosi and Desmarchelier 2019) and the characteristic Equation (9), we found that Zero Hopf bifurcations occur if $-C = 0$, $-A = 0$, and $B > 0$. They are equivalent with $d = \frac{bg[(f-g)S_1^*-(f+h)I_1^*-(f+h)}{[a(g-e)+m(g+h)]S_1^*+(bV_1^*-aI_1^*)gS_1^*+bhV_1^*}$, $d = -(gI_1^*+b+e+f+h)$, and $d > \frac{(fg-g^2)S_1^*-g(b+f+h)I_1^*-b(e+f+h)-e(f+h)}{gS_1^*V_1^*+(m-a)S_1^*+(b+h)V_1^*}$ where $gS_1^*V_1^* + (m-a)S_1^* + (b+h)V_1^* > 0$ respectively.

NUMERICAL SIMULATION

Susceptible-Coronavirus interaction rate (d), susceptible-infected interaction rate (g), infected subpopulation recovery rate (f), and Coronavirus increasing rate from infected subpopulation (a) vary numerically by using MATCONT (Wiraya and Adi-Kusumo 2023; Adi *et al.* 2023), then the impact of the variations in the dynamics of Covid-19 transmission in the population that become the characteristics of the transmission is identified. We set initial parameter values as written in Table 2.

Fold and Hopf Bifurcations

Continuation of $E_2 = (12.12660541, 1753.700767, -8.647237780)$ as susceptible-Coronavirus interaction rate (d) decreases generates a Fold bifurcation and three Hopf bifurcations which consist of two neutral saddle and one non-neutral saddle Hopf bifurcations, see Figure 2.

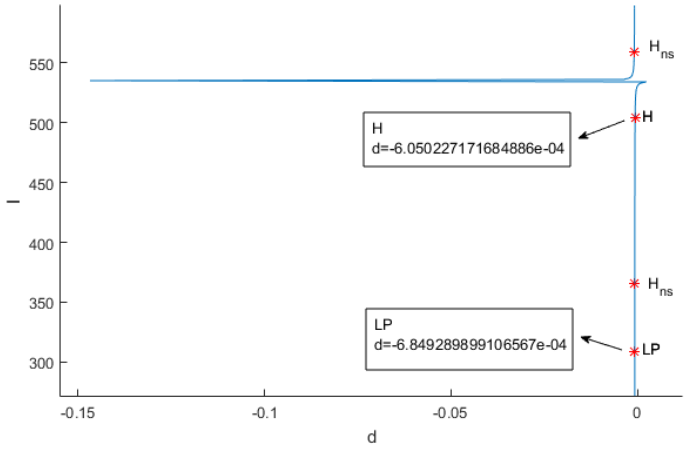

Figure 2 Bifurcation diagram generated by continuing E_2 as susceptible-Coronavirus interaction rate (d) decreases.

Two infection equilibrium points collide at the Fold bifurcation point and vanish when the prevention of Coronavirus infection through non-living objects has the same rate as the infection. A cycle is found at the non-neutral saddle Hopf bifurcation point which represents a fluctuation cycle of Coronavirus, susceptible, and infected subpopulations when the rate of the infection by Coronavirus that exists in non-living objects is less than its prevention rate. We make a continuation of the non-neutral saddle Hopf

bifurcation point to generate some codimension-two bifurcations which are explained in the next section.

Generalized Hopf, Zero Hopf, and Bogdanov-Takens Bifurcations

Continuations of the non-neutral saddle Hopf bifurcation point as susceptible-Coronavirus interaction rate (d), susceptible-infected interaction rate (g), infected subpopulation recovery rate (f), and Coronavirus increasing rate from infected subpopulation (a) vary are conducted, see Figure 3, Figure 4, and Figure 5.

Continuation of the non-neutral saddle Hopf bifurcation point as susceptible-Coronavirus interaction rate (d) and susceptible-infected interaction rate (g) decrease generates two Generalized Hopf and one Bogdanov-Takens bifurcations, see Figure 3.

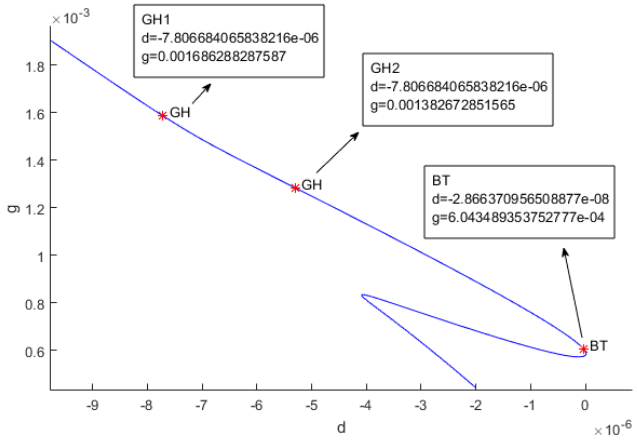

Figure 3 Bifurcation diagram generated by continuing the Fold point as susceptible-Coronavirus interaction rate (d) and susceptible-infected interaction rate (g) decrease.

The other codimension-two bifurcations are found by making continuation of the non-neutral saddle Hopf bifurcation point as the susceptible-Coronavirus interaction rate (d) decreases and infected subpopulation recovery rate (f) increases. It generates four Generalized Hopf, one Bogdanov-Takens, and two Zero Hopf bifurcations which consist of one non-neutral saddle and one neutral saddle Zero Hopf bifurcation, see Figure 4.

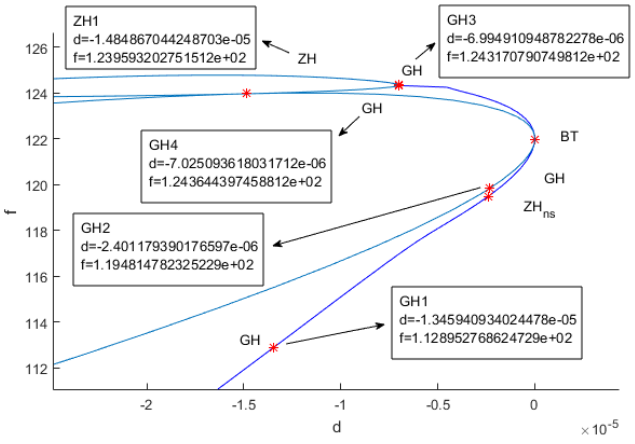

Figure 4 Bifurcation diagram generated by continuing the non-neutral Hopf bifurcation point as the Coronavirus interaction rate (d) decreases and the infected subpopulation recovery rate (f) increases.

We also make a continuation of the non-neutral saddle Hopf bifurcation point as susceptible-Coronavirus interaction rate (d) and Coronavirus increasing rate from infected subpopulation (a) decrease. It generates a Generalized Hopf bifurcation, see Figure 5.

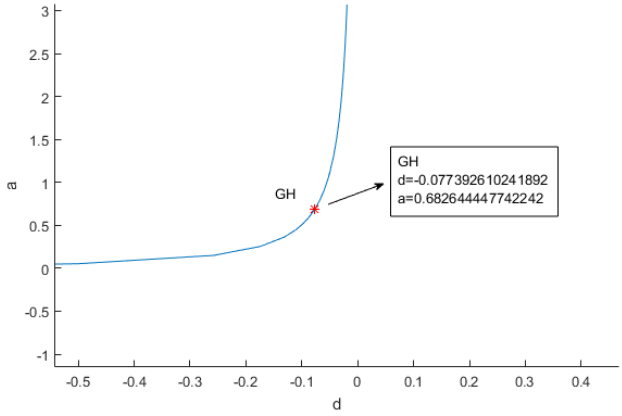

Figure 5 Bifurcation diagram generated by continuing the non-neutral Hopf bifurcation point as susceptible-Coronavirus interaction rate (d) and Coronavirus increasing rate from infected subpopulation (a) decrease.

Some phenomena are found around the Generalized Hopf bifurcation points, such as strange attractors and catastrophe which are discussed in the next section. The phenomena become some characteristics of Covid-19 transmission based on the varied parameters that can become an indicator to predict the dynamics of Covid-19 in the population.

Strange Attractors Generated by Generalized Hopf Bifurcations

We choose a value of (d, g) around the GH1 and GH2 points in Figure 3, and also (d, f) around the GH1 point in Figure 4. Then, we choose an initial value around the equilibrium which was found by choosing those parameters, then we found three strange attractors as shown in Figure 6(a), Figure 6(b), and Figure 6(c). We also calculate the Lyapunov exponent (Dieci *et al.* 1997) of the strange attractors to investigate their characteristic.

In Figure 6(a), we choose $(d, g) = (-7.806684065838216e-06, 0.001686288287587)$ around GH1 in Figure 3 and an initial value $(V, S, I) = (1.815098324208333e+04., 1.159155421086804e+03, 1.757552288703374e+02)$ generated by choosing those parameters. In Figure 6(b), we choose $(d, g) = (5.591353065874137e-06, 0.001482672851565)$ around GH2 in Figure 3 and an initial value $(V, S, I) = (1.918856995532746e+04, 1.125005746177521e+03, 1.862583288670330e+02)$ generated by choosing those parameters. In Figure 5, we choose $(d, f) = (-1.345940934024478e-05, 1.028952768624729e+02)$ around GH1 in Figure 4 and an initial value $(V, S, I) = (8.152543256535453e+03, 1.486804434008352e+03, 74.09169434849883)$ generated by choosing those parameters.

Lyapunov exponent of each variable generating the strange attractor shown in Figure 6(a), Figure 6(b), and Figure 6(c) are presented in Figure 6(c), Figure 6(d), and Figure 6(e) respectively. Based on the Lyapunov exponents, we found that all of the strange attractors are non-chaotic as all of the variable's Lyapunov exponents have a negative value (Wiraya and Adi-Kusumo 2023).

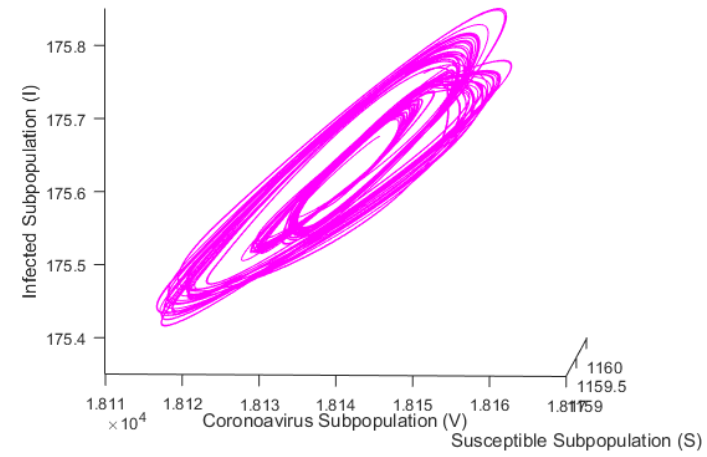

(a)

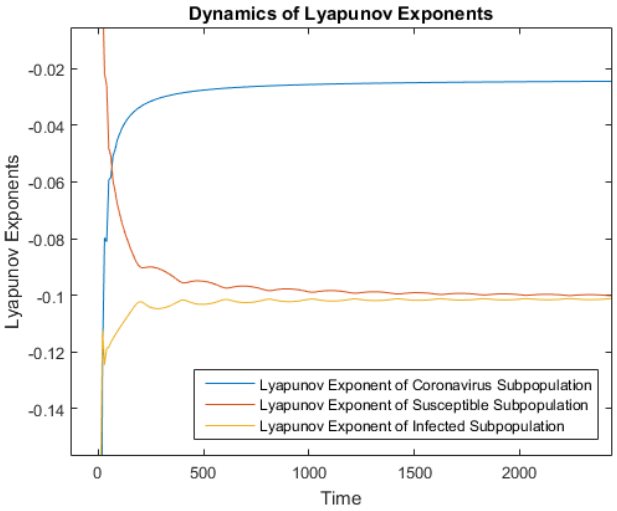

(d)

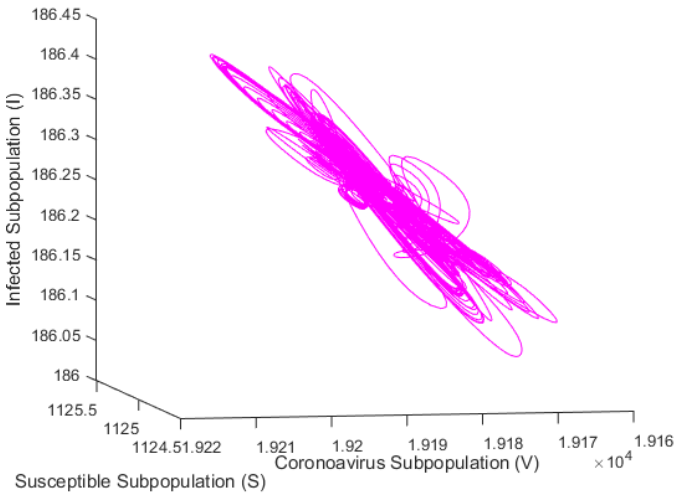

(b)

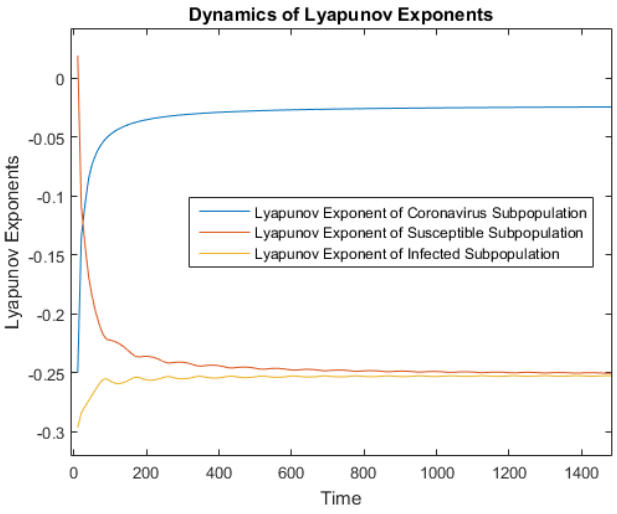

(e)

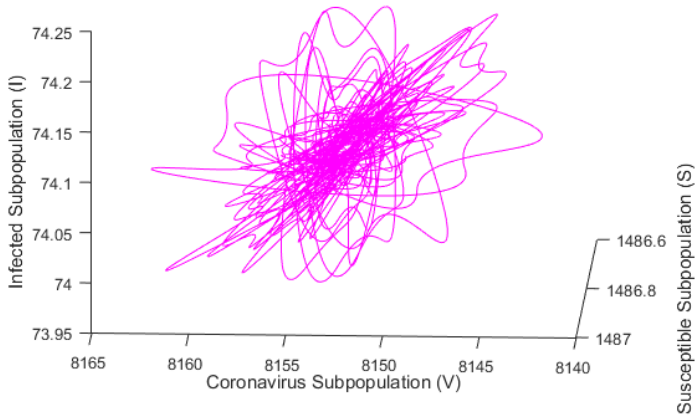

(c)

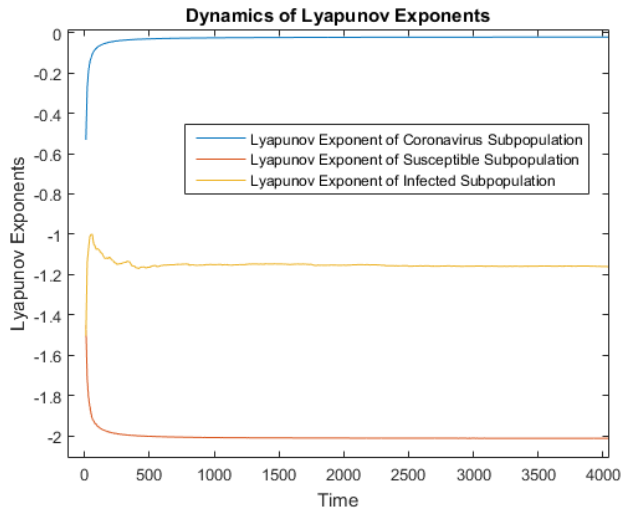

(f)

Figure 6 Strange attractors around GH1, GH2 in Figure 3 and GH1 in Figure 4 and the Lyapunov exponent of the variables which generate the strange attractors: (a) Strange attractor around GH1 in Figure 3, (b) Strange attractor around GH2 in Figure 3, (c) Strange attractor around GH1 in Figure 4, (d) Lyapunov exponent of the strange attractor around GH1 in Figure 3, (e) Lyapunov exponent of the strange attractor around GH2 in Figure 3, (f) Lyapunov exponent of the strange attractor around GH1 in Figure 4

The non-chaotic strange attractors represent a complex but predictable fluctuation of Coronavirus, susceptible, and infected subpopulations (Wiraya and Adi-Kusumo 2023) as one of the following variations occurs: i) susceptible-Coronavirus and susceptible-infected interaction rate decrease; ii) susceptible-Coronavirus interaction rate decrease and infected subpopulation recovery rate increases; iii) susceptible-Coronavirus interaction rate and Coronavirus increasing rate from infected subpopulation decrease.

Catastrophe Phenomenon

We choose a value of (d, a) around the GH point in Figure 5 and an initial value around the equilibrium found by choosing those parameters. Then, we found a catastrophe phenomenon generated by the attractor and repeller of the solution started by a smooth solution and then colliding at a region having a transformation of the solution pattern become chaotic confirmed by the Lyapunov exponent of each variable generates the attractor and repeller. The catastrophe phenomenon is presented in Figure 7 and Figure 8.

We choose $(d, a) = (-0.077392610241892, 0.682644447742242)$ around GH and an initial value $(V, S, I) = (3.943299602340211e+02, 1.020277404117016e+02, 5.026599969563091e+02)$ generated by choosing those parameters. Then, we plot the solution for forward time generating an attractor and backward time generating a repeller after a smooth solution. The attractor and repeller collide at a region constructing the chaotic part of the catastrophe phenomenon as shown in Figure 7. Chaotic part of the catastrophe phenomenon is presented in Figure 8.

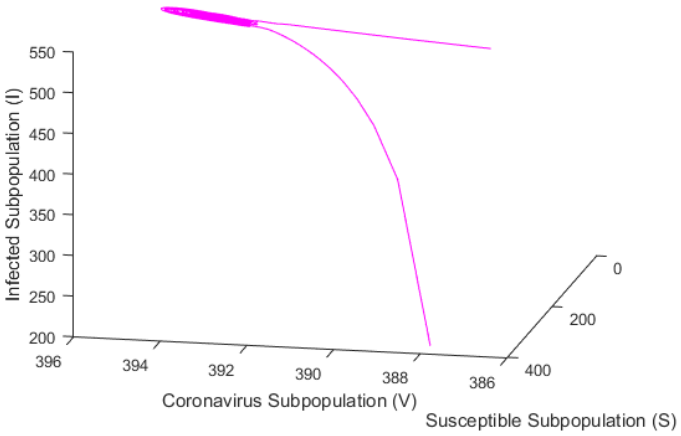

Figure 7 Catastrophe phenomenon around GH

Lyapunov exponent of each variable which generates the attractor and repeller is calculated to confirm the transition of the solution pattern from smooth to chaotic and vice versa. Calculations of the Lyapunov exponent of each variable which generates the attractor and repeller are presented in Figure 9 and Figure 10 respectively.

We investigate the catastrophe phenomenon further through the Lyapunov exponents of the variables in the attractor and repeller, especially the existence of their transition from negative to positive value which represents the transformation of the solution pattern. We found that the attractor and repeller are chaotic as the Lyapunov exponents of Coronavirus have a positive value (Wiraya and Adi-Kusumo 2023; Cencini *et al.* 2009) as time goes by, but they have a momentary negative value (dashed black circle) which

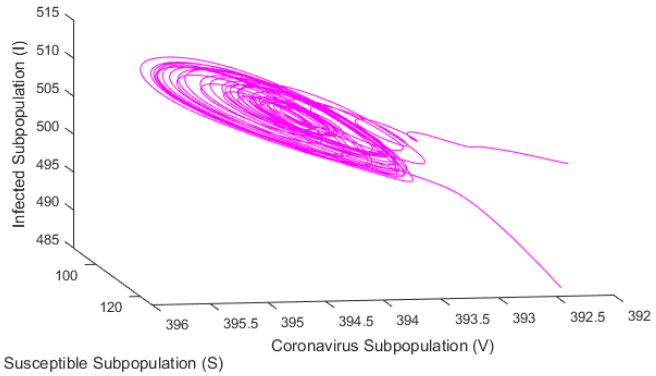

Figure 8 Chaotic part of the catastrophe phenomenon around GH

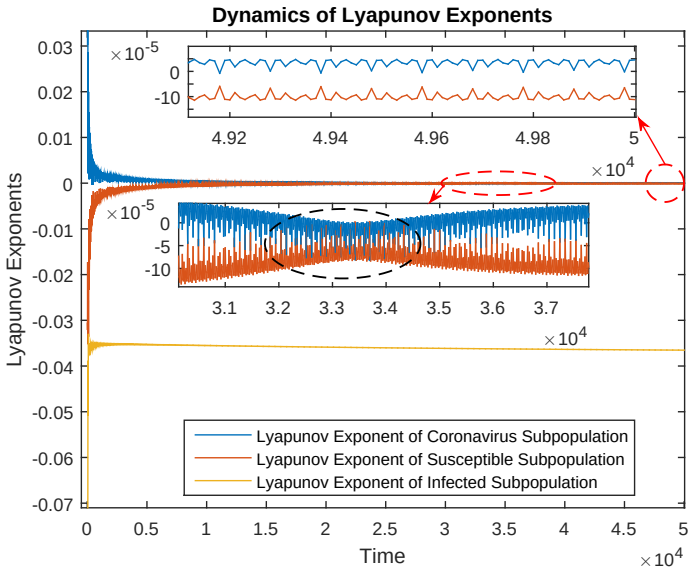

Figure 9 Lyapunov exponent of the variables in the attractor of the catastrophe phenomenon around GH

represents the smooth solution before they tend to a positive value. These phenomena illustrate the transformation of the solution pattern, i.e. smooth-chaotic-smooth solution which represents the catastrophe phenomenon.

Fluctuation of Coronavirus, susceptible, and infected subpopulations that start from a smooth, then change to a chaotic, then change back to a smooth pattern indicates the appearance of catastrophe phenomenon which represents a momentary complex and unpredictable fluctuation of them as susceptible-Coronavirus interaction rate Coronavirus increasing rate from infected subpopulation decrease.

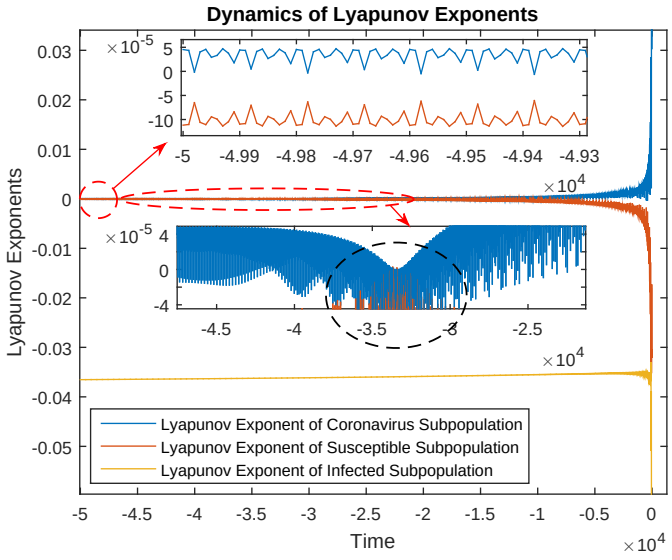

Figure 10 Lyapunov of the variables in the repeller of the catastrophe phenomenon around GH.

CONCLUSION

A three-dimensional ordinary differential equation system has been constructed as a new mathematical model of Covid-19 transmission in the population by considering two factors, i.e. non-living objects as one of the Coronavirus transmission media together with the susceptible subpopulation as one of the Coronavirus carriers. The model represents interactions between Coronavirus that exists on non-living objects, susceptible, and infected subpopulations. Analysis of the model reveals some results, such as equilibrium points along with their local stability and bifurcation analysis which consists of the finding of many interesting phenomena.

One disease-free and two infection equilibrium points are found in the model. The disease-free equilibria describes extinction of Coronavirus infection, so that the population is free from Covid-19. The infection equilibrium points describe the existence of Coronavirus infection in the population. Local stability conditions of disease-free equilibria should be fulfilled in order to make the population free from Covid-19 when initial subpopulations are around the disease-free equilibria. The population can also be free from Covid-19 for any initial condition of the subpopulations if the global stability conditions of the disease-free equilibria are fulfilled. Local stability conditions of infection equilibrium points should not be fulfilled so that Coronavirus infection in the population can be avoided when initial subpopulations are around the infection equilibrium points.

Codimension-one and codimension-two bifurcation analysis of the model gives some results that have a related biological meaning so they become some characteristics of Coronavirus transmission in the population relative to the parameter variations. Codimension-one bifurcation analysis has some results, i.e. the finding of Fold and non-neutral saddle Hopf bifurcation. Two infection equilibrium points collide at the Fold bifurcation point and then they vanish when the prevention of Coronavirus infection through non-living objects has the same rate as the infection. A cycle is found at the non-neutral saddle Hopf bifurcation point which represents a fluctuation cycle of Coronavirus, susceptible, and infected subpopulation when the eradication of Coronavirus by susceptible subpopulation is more vigorous than the infection.

Codimension-two bifurcation analysis shows that the model undergoes Generalized Hopf bifurcations. Those bifurcations trigger rich dynamics, i.e. strange attractors and catastrophe phenomena. Strange attractors which represent some complex and predictable fluctuation of Coronavirus, susceptible, and infected subpopulations are found as the susceptible-Coronavirus interaction rate decreases and one of these two variations occurs, i.e. susceptible-infected interaction rate decreases or the infected subpopulation recovery rate increases. Catastrophe phenomenon which represents a momentary complex and unpredictable fluctuation of Coronavirus, susceptible, and infected subpopulation is found as susceptible-Coronavirus interaction rate Coronavirus increasing rate from infected subpopulation decrease.

We also found some other codimension-two bifurcations, such as Bogdanov-Takens and Zero Hopf bifurcations. Bogdanov-Takens bifurcation has the potential to trigger the existence of homoclinic orbit or homoclinic bifurcations (Wiraya *et al.* 2024). Zero Hopf bifurcation can also become a trigger for strange attractor or repeller occurrence. Those two phenomena can become chaotic dynamics indicators. But recently, we still have not found those phenomena in this research. Therefore, investigation of homoclinic orbit and homoclinic bifurcations that can be triggered by the Bogdanov-Takens bifurcation, and also strange attractor or repeller that can be generated by the Zero Hopf bifurcation are our future research directions.

Acknowledgments

We would like to express our gratitude to Universitas Sebelas Maret who has funded this research through "Hibah Penelitian dan Pengabdian kepada Masyarakat (P2M) Penerimaan Negara Bukan Pajak (PNBP) Universitas Sebelas Maret 2023 (228/UN27.22/PT.01.03/2023)".

Availability of data and material

Not applicable.

Conflicts of interest

The authors declare that there is no conflict of interest regarding the publication of this paper.

Ethical standard

The authors have no relevant financial or non-financial interests to disclose.

LITERATURE CITED

Adi, Y., N. Irsalinda, A. Wiraya, S. Sugiyarto, and Z. Rafsanjani, 2023 Mathematical Modeling and Computing **10**: 311–325, DOI: 10.23939/mmc2023.02.311.

AlQadi, H. and M. Bani-Yaghoub, 2022 Incorporating global dynamics to improve the accuracy of disease models: Example of a covid-19 sir model. PloS one **17**: e0265815, DOI: 10.1371/journal.pone.0265815.

Bosi, S. and D. Desmarchelier, 2019 Local bifurcations of three and four-dimensional systems: A tractable characterization with economic applications. Mathematical Social Sciences **97**: 1–1, DOI: 10.1016/j.mathsocsci.2018.11.001.

Carraturo, F., C. Giudice, M. Morelli, V. Cerullo, G. Libralato, *et al.*, 2020 Persistence of sars-cov-2 in the environment and covid-19 transmission risk from environmental matrices and surfaces. Environmental Pollution **265**, DOI: 10.1016/j.envpol.2020.

Castillo-Garsow, C. and C. Castillo-Chavez, 2020 *A tour of the basic reproductive number and the next generation of researchers*. Springer International Publishing, Berlin/Heidelberg, Germany.

Cencini, M., F. Cecconi, and A. Vulpiani, 2009 *Chaos: from Simple Models to Complex Systems*. World Scientific, Singapore.

Dieci, L., R. Russell, and E. Van Vleck, 1997 SIAM Journal on Numerical Analysis **34**: 402–423, https://api.semanticscholar.org/CorpusID:18204582.

Din, R. and E. Algehyne, 2021 Mathematical analysis of covid-19 by using sir model with convex incidence rate. Results in Physics **23**, DOI: 10.1016/j.rinp.2021.103970.

for Disease Prevention, E. C. and Control, 2020 Using face masks in the community reducing covid-19 transmission from potentially asymptomatic or pre-symptomatic people through the use of face masks. Technical report, Stockholm.

Gandhi, M., D. Yokoe, and D. Havlir, 2020 Asymptomatic transmission, the achilles' heel of current strategies to control covid-19. The New England Journal of Medicine **382**: 2158–2160, DOI: 10.1056/NEJMe2009758.

He, F., Y. Deng, and W. Li, 2020 Coronavirus disease 2019: What we know? Journal of Medical Virology **92**: 719–725, DOI: 10.1002/jmv.25766.

Kuznetsov, Y., 1998 *Element of Applied Bifurcation Theory*. Springer-Verlag, Inc., New York.

LaSalle, J. and S. Lefschetz, 1961 *Stability by Lyapunov's Direct Method with Applications*. Academic Press, New York.

Mondal, B., A. Thirthar, N. Sk, M. Alqudah, and T. Abdeljawad, 2024 Complex dynamics in a two species system with crowley–martin response function: Role of cooperation, additional food and seasonal perturbations. Mathematics and Computers in Simulation **221**: 415–434, DOI: 10.1016/j.matcom.2024.03.015.

Obi, O. and D. Odoh, 2021 Transmission of coronavirus (sars-cov-2) by presymptomatic and asymptomatic covid-19 carriers? European Journal of Medical and Educational Technologies **14**, DOI: 10.30935/ejmets/11060.

Pakhira, R., B. Mondal, A. Thirthar, M. Alqudah, and T. Abdeljawad, 2024 Developing a fuzzy logic-based carbon emission cost-incorporated inventory model with memory effects. Ain Shams Engineering Journal p. 102746, DOI: 10.1016/j.asej.2024.102746.

Pedersen, S. and Y. Ho, 2020 Sars-cov-2: a storm is raging. The Journal of Clinical Investigation **130**: 2202–2205, DOI: 10.1172/JCI137647.

Perko, L., 2001 *Differential Equations and Dynamical Systems*. Springer-Verlag, Inc., New York, NY.

Ramesh, N., A. Siddaiah, and B. Joseph, 2020 Tackling coronavirus disease 2019 (covid 19) in workplaces. Indian Journal of Occupational and Environmental Medicine **24**: 16–18.

Sender, R., Y. Bar-On, S. Gleizer, B. Bernshtein, A. Flamholz, *et al.*, 2021 The total number and mass of sars-cov-2 virions. Proceedings of the National Academy of Sciences of the United States of America **118**, DOI: 10.1073/pnas.2024815118.

Sk, N., B. Mondal, A. Thirthar, M. Alqudah, and T. Abdeljawad, 2023 Bistability and tristability in a deterministic prey–predator model: Transitions and emergent patterns in its stochastic counterpart. Chaos, Solitons and Fractals **176**: 114073, DOI: 10.1016/j.matcom.2024.03.015.

Thirthar, A., 2023 A mathematical modelling of a plant-herbivore community with additional effects of food on the environment. Iraqi Journal of Science **64**: 3551–3566, DOI: 10.24996/ijs.2023.64.7.34.

Thirthar, A., N. Sk, B. Mondal, M. Alqudah, and T. Abdeljawad, 2023 Utilizing memory effects to enhance resilience in disease-driven prey-predator systems under the influence of global warming. Journal of Applied Mathematics and Computing **69**: 4617–4643, DOI: 10.1007/s12190-023-01936-x.

van Doremalen, N., T. Bushmaker, D. Morris, M. Holbrook, A. Gamble, *et al.*, 2020 Aerosol and surface stability of sars-cov-2 as compared with sars-cov-1. The New England Journal of Medicine **382**: 1564–1567, DOI: 10.1056/NEJMc2004973.

Verhulst, F., 1996 *Nonlinear differential equation and dynamical systems*. Springer-Verlag, Inc., New York.

Vermund, S. and V. Pitzer, 2021 Asymptomatic transmission and the infection fatality risk for covid-19: Implications for school reopening. Clinical Infectious Diseases **7**: 1493–1496, DOI: 10.1093/cid/ciaa855.

WHO, 2020 Website of the who coronavirus (covid-19) dashboard. Technical report, World Health Organization.

Wiggins, S., 2003 *Introduction To Applied Nonlinear Dynamical Systems And Chaos*. Springer-Verlag, Inc., New York.

Wiraya, A., Y. Adi, L. Fitriana, Triyanto, and S. Khoirunnisa, 2022 Global stability of latency equilibria on mathematical model for human inflammatory response to coronavirus infection. In *Internationa Conference of Mathematics and Mathematics Education (I-CMME) 2021, I-CMME 2021, Surakarta, Indonesia*, pp. 030009–1–030009–9.

Wiraya, A. and F. Adi-Kusumo, 2023 Torus and homoclinic bifurcations on a cells repair regulations model of the metastatic nasopharyngeal carcinoma. Journal of Nonlinear Science **33**: 1–21, DOI: 10.1007/s00332-023-09925-x.

Wiraya, A., L. Fitriana, Triyanto, Y. Adi, Y. Kusumadewi, *et al.*, 2024 Bifurcation analysis of the dynamics in covid-19 transmission through living and nonliving media. Journal of Applied Mathematics **2024**: 1–15, DOI: 10.1155/2024/5669308.

Yang, C. and J. Wang, 2020 A mathematical model for the novel coronavirus epidemic in wuhan, china. Mathematical Biosciences and Engineering **17**: 2708–2724, DOI: 10.3934/mbe.2020148.

Zu, Z., M. Jiang, P. Xu, W. Chen, Q. Ni, *et al.*, 2020 Coronavirus disease 2019 (covid-19): A perspective from china. Radiology **296**: E15–E25, DOI: 10.1148/radiol.2020200490.

How to cite this article: Wiraya, A., Adi, A. Y., Fitriana, L., Triyanto., Kusumadewi, Y. A., Safitri, A. N., and Nurmalitasari, A. Birth of Catastrophe and Strange Attractors through Generalized Hopf Bifurcations in Covid-19 Transmission Mathematical Model. *Chaos Theory and Applications*, 6(3), 159-169, 2024.